Research Square

Preprints are preliminary reports that have not undergone peer review.
They should not be considered conclusive, used to inform clinical practice,
or referenced by the media as validated information.

Enzymatic Degradation Behavior of Cotton, Lyocell, and Wood Pulp

Jeongmin Oh
North Carolina State University
Eunkyoung Shim
North Carolina State University
Sonja Salmon
sisalmon@ncsu.edu

North Carolina State University

Research Article

Keywords: Cellulose, enzyme, fiber, morphology, recycle, textile

Posted Date: November 24th, 2026

DOI: https://doi.org/10.21203/rs.3.rs-11145345/v1

License: This work is licensed under a Creative Commons Attribution 4.0 International License.
Read Full License

Additional Declarations: No competing interests reported.

Enzymatic Degradation Behavior of Cotton, Lyocell, and Wood Pulp

Jeongmin Oh[1], Eunkyoung Shim[1,*], Sonja Salmon[1,*]

[1]*Department of Textile Engineering, Chemistry and Science, Wilson College of Textiles, North Carolina State University, Raleigh, NC 27695-8301, USA*

*Corresponding Authors: Eunkyoung Shim, E-mail: eshim@ncsu.edu; Sonja Salmon, E-mail: sisalmon@ncsu.edu

Abstract

The widespread use of cellulose fibers in textile and nonwoven materials has increased interest in enzymatic degradation for sustainable recycling and waste management. However, comparatively less attention has been given to understanding how structural differences among cellulose fiber types influence enzyme accessibility and fragmentation behavior. In this study, the enzymatic degradation behavior of three structurally distinct and commercially important cellulose fibers, raw cotton, lyocell, and wood pulp, was investigated under identical hydrolysis conditions with and without alkaline pretreatment. Gravimetric analysis, scanning electron microscopy (SEM), X-ray diffraction, and fiber quality analysis were used to evaluate degradation efficiency and fiber fragmentation characteristics. Cotton exhibited the fastest degradation due to its twisted ribbon-like morphology and high enzyme accessibility, whereas lyocell showed limited initial degradation but became highly susceptible following alkaline pretreatment through enhanced swelling and fibrillation. In contrast, wood pulp showed the greatest resistance to enzymatic degradation because its collapsed, hornified, and highly entangled morphology prompted fiber aggregation and limited enzyme accessibility. These results demonstrate that parameters of fiber structure and morphology, fibrillar organization, and mixing behavior are critical factors in enzymatic degradation that extend beyond crystallinity alone. The mechanistic understanding established in this study provides a framework for predicting fiber-dependent degradation behavior and supports the design of enzymatic degradation processes for textile recycling and nonwoven waste management.

Acknowledgements

The authors thank Audrey Kim for assistance with experimental work and Luz Meza Carvajal for assistance with FQA measurements. We also thank Novonesis for providing the enzyme used in this study.

Keywords: Cellulose, cotton, lyocell, wood pulp, enzyme, recycle

Graphical Abstract

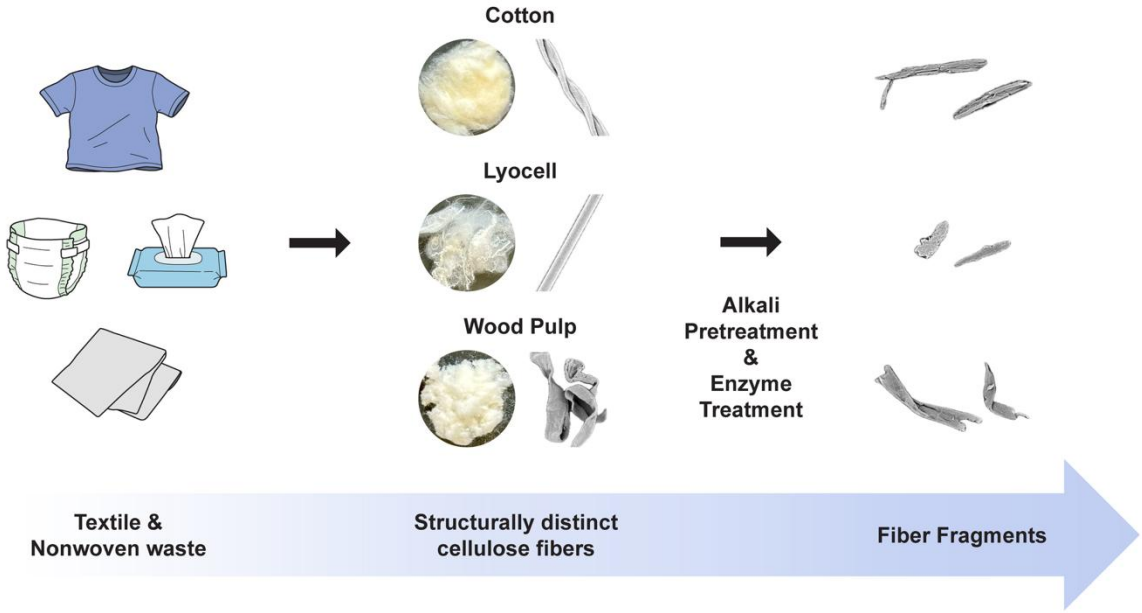

Introduction

Cellulose fibers are widely used in both textile and nonwoven materials due to their excellent absorbency, wet strength, and inherent biodegradability, which make them important for sustainable and disposable material applications (Santos et al. 2021). However, the lifecycle of cellulose fibers differs significantly between the two material systems. Conventional textile applications primarily utilize cotton and manufactured cellulose fibers in woven or knitted fabrics intended for extended use. Nonwoven materials frequently use wood pulp, cotton, and manufactured cellulosic as a bio-based source in single-use disposable hygiene and absorbent products such as diapers and wipes. Wood-derived fluff pulp is typically produced from bleached softwood kraft pulp and is designed to form a bulky and highly absorbent fiber structure. Although native softwood contains approximately 25-30 % lignin (Smook 2016), kraft pulping and bleaching remove most of the lignin while preserving the native cellulose fiber morphology, producing a cellulose-rich material that is particularly important in absorbent nonwovens due to its high fluid retention capacity and swelling behavior (Kakonke et al. 2019). Lyocell, a manufactured solution-spun cellulosic fiber, is usually produced from dissolving pulp derived from wood (Jiang et al. 2020). Here too, the natural lignin has been extracted, leaving an almost pure cellulose material that (Jiang et al. 2020), upon solubilization, loses its native morphology and recrystallizes during the fiber formation process (Zhang et al. 2018). Cotton fibers do not contain lignin and are ~95% pure cellulose at harvest (Wakelyn et al. 2006). However, raw cotton fibers are protected by a primary cell wall comprising pectins and waxes that impart hydrophobicity and lubricity. Some nonwoven products use cotton in its raw form, absent scouring and bleaching that removes the primary cell wall during conventional textile processing. Therefore, raw cotton, fluff pulp and lyocell fibers represent a broad range of morphological characteristics, while each are almost entirely composed of cellulose polymer, and each are utilized in various nonwoven materials.

Increasing production and consumption of textile and nonwoven materials have intensified challenges associated with cellulose-containing waste. Plant-based and manmade cellulosic fibers together accounted for approximately 39.7 million tonnes, representing 30% of global fiber production in 2024 (Textile Exchange 2025). Meanwhile, global nonwoven consumption reached approximately 16.1 million tonnes in 2025 and is expected to increase to 21.5 million tonnes by 2030 (Smithers 2025). Synthetic polymers, primarily polypropylene, dominate nonwoven raw materials, while wood pulp and viscose accounted for approximately 11% and 6%, respectively, of reported raw-material consumption in 2017 (EDANA 2019). Consequently, efficient degradation of cellulose fibers offers important opportunities for nonwoven waste management and textile recycling. Understanding the biodegradation behavior of nonwoven cellulose materials is important not only for exploring degradation mechanisms but also for guiding material selection and recycling strategies for disposable nonwoven products.

Conventional recycling and degradation approaches for cellulose fiber-based materials typically involve mechanical or chemical processing. Mechanical recycling is widely implemented because of its scalability, but repeated processing often causes fiber shortening and a decrease in fiber quality (Huang et al. 2024). As a result, selective degradation and chemical separation strategies have been explored for cellulose-based materials where conventional mechanical recycling is difficult. For example, in textile recycling, mechanical separation of cellulose fibers from polyethylene terephthalate (PET) fibers in blended yarns is impossible due to tightly entangled fiber components. Chemical PET separation approaches include solvent-based dissolution and depolymerization processes such as glycolysis, alkali hydrolysis, and enzymatic hydrolysis (Enking et al. 2025). Meanwhile, cellulose removal has been investigated using solvent systems including ionic liquids/DMSO-based systems (De Silva et al. 2014; Zhang et al. 2017), N-methylmorpholine-N-oxide (NMMO) (Jeihanipour et al. 2010), alkali/urea systems (Liu et al. 2019), deep eutectic solvents (DESs) (Yang et al. 2024) and enzymatic hydrolysis (Egan et al. 2023). Acidic hydrolysis has also been explored as an alternative pathway for cellulose removal and depolymerization (Ruiz-Caldas et al. 2022; Costa et al. 2022). Although these approaches were developed for textile recycling applications, growing demand for sustainable and renewable materials has increased interest in utilizing cellulose fibers in nonwoven products even though synthetic fibers still account for the majority of nonwoven production (EDANA 2019). Nonwoven materials consist of interconnected fiber networks in sheet form, suggesting that degradation strategies developed for conventional textiles may also be relevant to nonwoven materials. However, cellulose fibers used in nonwovens often differ in processing history and morphology, which can strongly influence degradation behavior. As a result, further investigation of cellulose fibers relevant to nonwoven applications is needed to better understand fiber-dependent degradation mechanisms.

Among selective degradation approaches, enzymatic degradation of cellulose is a highly selective strategy for cellulose removal and material separation that offers sustainability benefits (Li et al. 2019; Kaabel et al. 2023). Natural cellulase enzymes include multiple components, including endoglucanase, cellobiohydrolases, and β-glucosidases, that work together to hydrolyze glycosidic bonds within cellulose chains, with endoglucanases primarily attacking accessible amorphous cellulose regions, cellobiohydrolases breaking down cellulose chain ends, and β-glucosidases hydrolyzing cellobiose into glucose (Zhang and Lynd 2004) (**Fig. 1**). Enzymatic hydrolysis of cellulose has long been utilized in biomass conversion, where the primary objective is complete saccharification of cellulosic or lignocellulosic materials into glucose for applications such as biofuel production (Cho et al. 2023) and this approach has also been explored for cotton textile waste in combination with mechanical refining (Vera et al. 2023) or alkaline pre-treatment (Simonetti et al. 2024). However, for waste management applications, complete hydrolysis of cellulose is not necessarily required.

Instead, controlled fragmentation of cellulose into sufficiently small particles that can be dispersed and removed through liquid separation may provide an alternative pathway for cellulose removal (Egan et al. 2023). Consequently, understanding fiber fragmentation behavior and residual fragment characteristics during enzymatic hydrolysis is important, alongside evaluating overall weight loss.

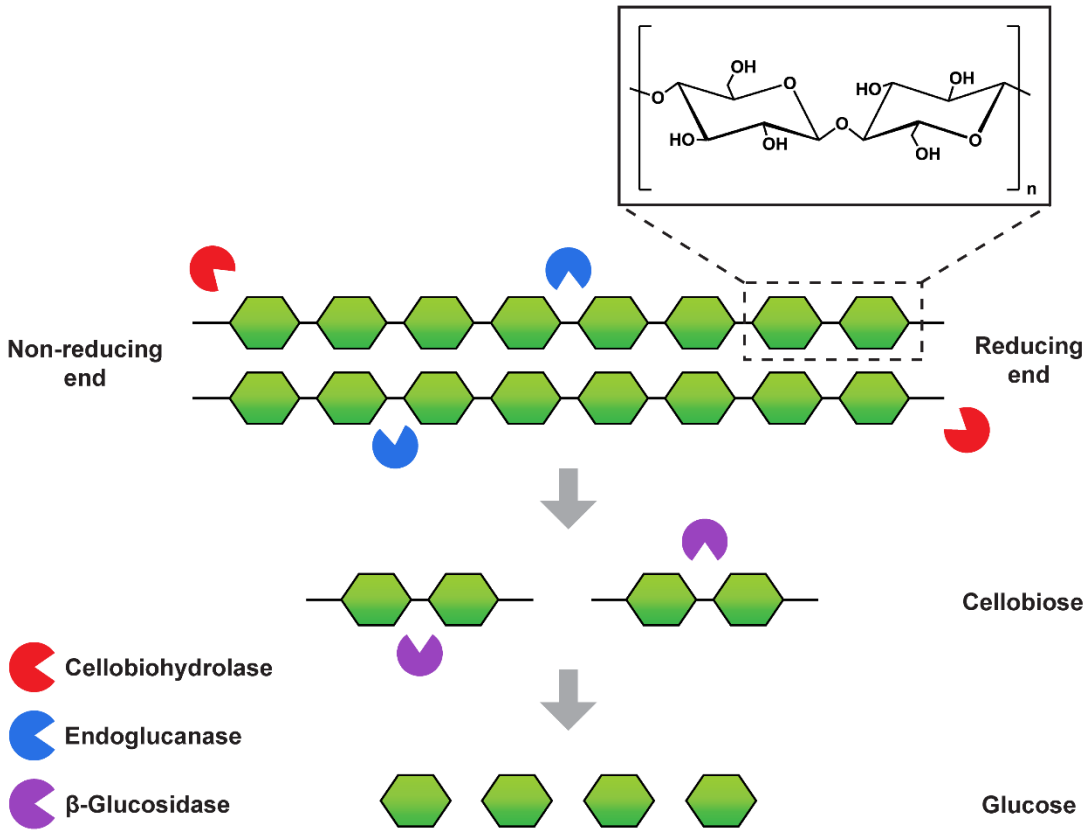

Fig. 1 Schematic illustration of cellulose hydrolysis by the cellulase enzyme

Despite significant attention on enzymatic cellulose degradation, most previous textile-related studies focus on single cellulose fiber types, typically the chemically processed cotton used in conventional textiles. Cotton fibers used in textile fabrics generally undergo scouring and bleaching to remove natural waxes and noncellulosic impurities to improve wettability and dyeing uniformity (Schindler and Hauser 2004). In contrast, nonwoven materials may instead utilize raw or minimally processed cotton fibers, particularly in applications where whiteness, dyeing uniformity, or extensive chemical processing are less critical (Nam et al. 2016). Although bleached cotton remains dominant in cotton-based nonwoven products (Nam et al. 2016), raw cotton has also been explored for nonwoven applications as it eliminates bleaching processes while maintaining sufficient absorbency after the hydroentanglement process (Sawhney et al. 2010). The mechanical properties of nonwoven materials are strongly

influenced by fiber structural characteristics (Hinchliffe et al. 2023), suggesting that differences in fiber processing history may also affect enzyme accessibility and degradation behavior. Accordingly, the remaining surface wax and impurities of raw cotton fibers can reduce wettability and are expected to restrict accessibility of the fiber surface to water and enzymes compared to chemically processed cotton fibers. Mechanically processed wood pulp fibers used in absorbent nonwovens also have distinct structural and morphological characteristics, including shorter fiber length and collapsed fiber structure, compared to textile-grade cellulose fibers. Nevertheless, comparatively less attention has been given to the direct comparison of structurally distinct cellulose fibers under identical conditions. As a result, the role of fiber-specific structural features in enzyme accessibility and fragmentation behavior remains insufficiently understood. Therefore, evaluating fiber-type dependent enzymatic degradation behavior is essential for identifying structural factors governing enzyme accessibility and fragmentation. The three cellulose fibers investigated in this study represent structurally distinct cellulose fibers that differ in origin, morphology, and processing history, as summarized in **Table 1**.

Table 1 Comparison of the characteristics of cotton, lyocell, and wood pulp fibers

Characteristics	Cotton	Lyocell	Wood Pulp
Source	Natural seed coat fiber	Solution-spun manufactured cellulose fiber	Bleached kraft “fluff” pulp
Applications	Textiles, nonwovens	Textiles, nonwovens	Absorbent nonwovens
Cellulose polymorph	Cellulose I	Cellulose II	Cellulose I
Fiber morphology	Twisted ribbon with lumen	Circular, smooth cross section	Short, collapsed flat ribbon
Typical fiber length	25-33 mm (Joseph 1986)	28-60 mm (commercial staple fibers) (Lenzing AG 2026)	2.5-7 mm (softwood tracheids) (Bajpai 2018)

Fiber length used in this study	28.3 mm	51 mm	1.3 mm
Processing history of fibers used in this study	Raw, unbleached	Solution-spun	Mechanical processing, bleached

Although cellulose fibers share an almost identical base chemical composition, their structural characteristics vary significantly depending on origin and processing history. Cotton, the most widely produced natural textile fiber (Textile Exchange 2025), consists primarily of cellulose I with parallel chain packing, strong hydrogen bonding, and relatively high crystallinity (Moon et al. 2011). Cotton fibers have a distinctive twisted ribbon-like morphology formed by the collapse of the lumen during fiber maturation and drying, resulting in a convoluted structure with high surface irregularity (Haigler et al. 2012). Cotton fiber cell walls exhibit a multilayered structure with varying microfibril orientations, including helically arranged fibrils in the transitional layer of the primary cell wall and more axially aligned fibrils within the secondary wall (Leenders et al. 2025). In contrast, lyocell is a solution-spun manufactured cellulose fiber produced through direct dissolution of cellulose in N -methyl morpholine-N-oxide (NMMO) solvent systems (Jiang et al. 2020), resulting in an antiparallel cellulose II crystal structure. Lyocell fibers exhibit a characteristic skin-core morphology, in which a thin outer skin, that is subject to fibrillation when abraded (Ma et al. 2021), surrounds a dense core (Abu-Rous et al. 2006). Compared to cotton and lyocell, wood-derived fluff pulp is typically produced from bleached softwood kraft pulp, which consists of tracheid fibers of approximately 2-5 mm in length depending on the wood species (Bajpai 2018). These mechanically processed cellulose I fibers undergo fiber wall collapse and hornification during drying and processing, resulting in flattened fiber morphology and reduced reopening of internal pore structures upon rewetting (Hubbe et al. 2007). Wood pulp fibers also exhibit layered secondary wall structures with varying microfibril orientations across wall layers, producing less uniform fibrillar organization than highly oriented manufactured cellulose fibers (Barnett and Bonham 2004). These differences in fiber morphology, crystalline structure, and fibrillar orientation are expected to influence swelling behavior, enzyme accessibility, and fragmentation mechanisms during enzymatic hydrolysis.

Pretreatment strategies, including alkaline and acid treatments, are commonly applied to enhance enzymatic hydrolysis by improving fiber accessibility and disrupting hydrogen bonding within cellulose structures. Acidic pretreatments have been

investigated for cellulose-based fiber materials, particularly cellulose/PET blends, where concentrated acids such as phosphoric acid can disrupt cellulose crystalline structure and allow efficient enzymatic hydrolysis while preserving PET fibers (Shen et al. 2013; Sasaki et al. 2020). Alkaline pretreatments are widely used to enhance enzymatic hydrolysis of cellulose materials by disrupting hydrogen bonding, reducing the degree of crystallinity, and increasing fiber accessibility (Ma et al. 2024). Depending on alkali concentration and treatment conditions, alkaline pretreatments can also induce structural rearrangements, including transformation between cellulose polymorphs, such as conversion of cellulose I to cellulose II during cotton mercerization (Isogai and Atalla 1998). Under controlled low treatment conditions, alkaline pretreatment can significantly improve hydrolysis efficiency while minimizing degradation of other material components, as demonstrated in cellulose/PET systems (Gritsch et al. 2023). While the effects of pretreatment on overall hydrolysis efficiency have been widely investigated (Boondaeng et al. 2023), comparatively less attention has been given to its effect on fragmentation behavior across different cellulose fiber types.

In this study, the enzymatic degradation behavior of three structurally distinct cellulose fibers, raw cotton, lyocell, and wood pulp, was systematically investigated under controlled conditions, both with and without alkaline pretreatment. Raw cotton and wood pulp were selected to represent minimally processed natural fibers and mechanically processed nonwoven cellulose materials, respectively, both of which differ substantially from conventional textile fiber materials in processing history and structure. Lyocell was selected to represent a cellulose fiber that no longer has its natural morphology due to chemical solubilization followed by resolidification. A multi-scale characterization approach was used to evaluate both the degradation extent and residual fiber fragment characteristics, including gravimetric analysis, structural characterization, and fiber size distribution. By correlating the intrinsic fiber structure with enzyme accessibility and fragmentation behavior, this work provides insight into fiber-dependent enzymatic degradation mechanisms and establishes a foundation for the design, selection, and selective removal of cellulose fibers in textile and nonwoven applications.

Materials and Methods

Materials

Unbleached, ultraclean raw cotton fibers (Wildwood Cotton Technologies, Greenwood, MS, USA) with a nominal fiber length of 28.3 mm, measured according to ASTM D5103 (ASTM 2018) (**Fig. S1**), were used. LENZING™ Lyocell fibers (1.7 dtex, 51mm fiber length) were obtained from Lenzing (Lenzing AG, Lenzing, Austria). Wood fluff pulp was manually extracted from a commercially available nonwoven hygiene product (Pampers diaper, Procter & Gamble, Cincinnati, OH, USA). The extracted fibers exhibited an arithmetic mean fiber length (Ln) of 1.3 mm (length weighted mean (L_{lw}) of 1.8 mm) as measured by Fiber quality analysis (FQA). Cellic™ CTec3, a multicomponent commercial cellulase, was provided by Novonesis (Bagsværd, Denmark). The enzyme batch activity was determined to be 164 FPU/ml using a downscaled filter paper unit assay (Egan et al. 2023). G6 Glass Fiber Circles (5.5cm diameter, 1.6 µm particle retention) were purchased from Fisher Scientific (Pittsburgh, PA, USA). Sodium hydroxide, glacial acetic acid, and sodium acetate were purchased from Fisher Scientific (Waltham, MA, USA). Deionized water was used in all experiments.

Methods

Enzymatic degradation of fibers

Before enzymatic treatment, cellulose fibers were rinsed three times with deionized water to pre-wet the bulky fibers and ensure complete wetting and uniform dispersion in the reaction buffer. The prewetting step was performed without chemical treatments to preserve the surface characteristics of the fibers. For each experiment, 0.5g of fiber was placed into a 250 mL capped glass bottle containing cellulase enzyme solution prepared in 100 mM sodium acetate buffer (pH 5.0) at a liquor ratio of 80:1. Two magnetic stir bars (50 mm straight and 40 mm egg-shaped) were added to each bottle to improve mixing efficiency during hydrolysis. The enzymatic degradation procedure, adapted from the method of Egan et al. (Egan et al. 2023), was conducted using a 2mag Stirring Drybath 15-250 (2mag-USA, Daytona Beach, FL, USA) at 50 °C and 500 rpm. Enzyme loadings of 0, 10, and 20 FPU/g (which corresponds to 0, 6, 12 wt% of dry cellulose fibers, respectively) were investigated.

After hydrolysis, the reaction mixture was separated into three fractions by filtration. Residual large solids (>2 mm) were first separated using a 2 mm stainless steel mesh screen. The remaining suspension was vacuum filtered using a G6 glass fiber filter to collect small solid fragments. The resulting fractions consisted of: (1) large solids (>2 mm), (2) small solid fragments (<2 mm), and clarified liquid with water-soluble degraded components (< 1.6 µm), calculated as weight loss. For alkaline pretreatment, each 0.5g fiber sample was treated individually in 75 mL 1 M NaOH

solution for 1 h under different temperature conditions: room temperature, cold treatment (-30 °C), and hot treatment (50 °C). Following pretreatment, fibers were thoroughly washed with deionized water until a neutral pH was reached before proceeding with the enzymatic hydrolysis procedure.

Characterization of Cellulose fibers and fiber fragments

The untreated fibers and residual fiber fragments after enzymatic hydrolysis were characterized to evaluate the extent of enzymatic degradation and changes in the physical and structural properties of the cellulose fibers and residual fiber fragments. Gravimetric analysis was used to quantify degradation. SEM, XRD, FQA, and FTIR were used to characterize morphological, crystalline, dimensional, and chemical changes of cellulose fibers under different treatment conditions, respectively.

Gravimetrical analysis

After separation of the reaction mixture into large solids, small solids, and clarified liquid, the residual large and small solids were dried and weighed. Dry weights were measured using a Mettler Toledo HC103 Moisture Analyzer (Mettler-Toledo, LLC, Columbus, OH 43240 USA) at 105 °C. Weight loss, which represents the amount of original material that was converted to water-soluble products, was calculated according to Eq. (1):

$$Weight\ Loss\ (\%) = \frac{M_I - (M_L + M_S)}{M_I} \times 100 \qquad (1)$$

where M_I is the initial fiber weight (g), M_L is the dry weight of residual large solids (g), and M_S is the dry weight of residual small solids (g).

Scanning electron microscopy (SEM)

Scanning electron microscopy (SEM) was performed using a TM4000-Plus Tabletop Microscope (Hitachi High-Tech Corporation, Tokyo, Japan) operated at accelerating voltages of 10 and 15 kV. Residual small solid samples collected after enzymatic degradation were dried and mounted onto stainless steel specimen holders using conductive double-sided carbon adhesive tape. Samples were sputter-coated with gold using a vacuum sputter-coater (Emitech SC7620 Sputter Coater) to improve electrical conductivity before imaging.

X-ray diffraction (XRD)

For X-ray diffraction (XRD), scanning was performed at room temperature with an X-ray diffractometer (Rigaku SmartLab X-ray Diffractometer, Tokyo, Japan), with main parameter settings of: v = 40 kV, I = 44 mA, CuK α1 radiation source (λ = 1.5406 Å), Step Scan Mode, 2θ range = 10°-40° with a step of 0.05°. Scanning was performed at room temperature. The percent crystallinity (X_c) was calculated based on the areas under crystalline and amorphous peaks (Hermans and Weidinger 1961), according to Eq. (2):

$$X_c\ (\%) = \frac{A_c}{A_c + A_a} \times 100 \qquad (2)$$

where A_c and A_a represent the integrated areas corresponding to crystalline and amorphous regions, respectively. The empty sample holder was scanned to subtract the background noise from the measured diffraction patterns prior to peak integration analysis.

Fiber quality analysis (FQA)

Fiber fragment size distribution of residual small solids was measured using a Fiber Quality Analyzer (FQA-360, Code LDA17, OpTest Equipment Inc., Hawkesbury, ON, Canada). A small portion of the residual fiber suspension was diluted in approximately 600 mL of deionized water to obtain an appropriate fiber concentration for testing. Arithmetic mean fiber length (L_n) and length-weighted mean fiber length (L_{lw}) were calculated according to Eqs. (3) and (4), respectively:

$$Arithmetic\ length\ (\mathrm{L}_n) = \frac{\sum n_i l_i}{\sum n_i} \qquad (3)$$

$$Length\ Weighted\ length\ (\mathrm{L}_{lw}) = \frac{\sum n_i {l_i}^2}{\sum n_i l_i} \qquad (4)$$

where n_i is the number of fibers within a given length category, and l_i is the corresponding fiber length. As the arithmetic mean length (L_n) is strongly influenced by the presence of fines, the length weighted mean (L_{lw}) provided reduced sensitivity to fines and greater emphasis on longer residual fragments (OpTest Equipment Inc. 1996-2012). The FQA measurement range defines fibers between 0.04-15 mm, with fibers in the 0.04-0.2 mm range classified as fines.

Fourier-transform infrared (FTIR) spectroscopy

Fourier-transform infrared (FTIR) spectroscopy was performed using a Thermo Fisher Nicolet iS10 FT-IR spectrometer equipped with a Germanium (Ge) crystal

sampling head. A total of 64 scans at a resolution of 4 cm^{-1} were collected for each sample in the range of 400 - 4000 cm^{-1}.

Results and discussion

The degradation behavior of cellulose fiber is governed by multiple structural factors rather than a single fiber characteristic or property. As summarized in **Fig. 2**, fiber morphology, fibrillar structure, mixing behavior, and crystalline structure collectively influence enzyme accessibility, fragmentation behavior, and hydrolysis efficiency. Cotton, lyocell, and wood pulp exhibit distinct degradation behavior resulting from differences in their fiber structures. The following sections examine these structural characteristics and degradation behaviors to explain the observed fiber structure-dependent degradation mechanism.

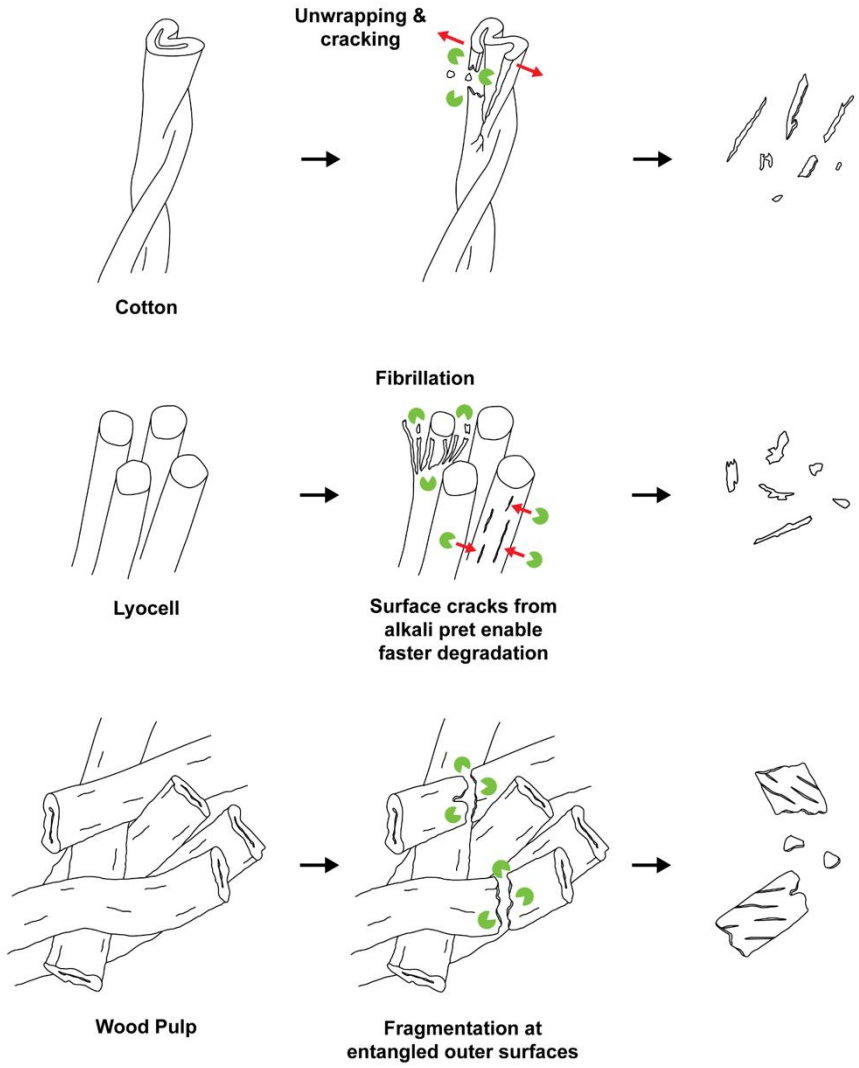

Fig. 2 Observed fiber structure-dependent enzymatic degradation mechanism of cellulose fibers. Cotton exhibits high enzyme accessibility due to its twisted ribbon-like morphology and lumen structure, allowing rapid unwrapping, fibrillation, and hydrolysis. Lyocell initially exhibits limited enzyme accessibility because of its smooth surface and densely packed fibrillar structure, but alkali pretreatment disrupts the outer skin and promotes swelling and fibrillation, resulting in greatly enhanced hydrolysis. Wood pulp is characterized by a collapsed or hornified, flat ribbon-like, and highly entangled morphology that promotes fiber aggregation, restricts enzyme accessibility, and results primarily in fiber fragmentation with limited fibrillation.

Fiber Type Dependent Enzymatic Degradation Behavior

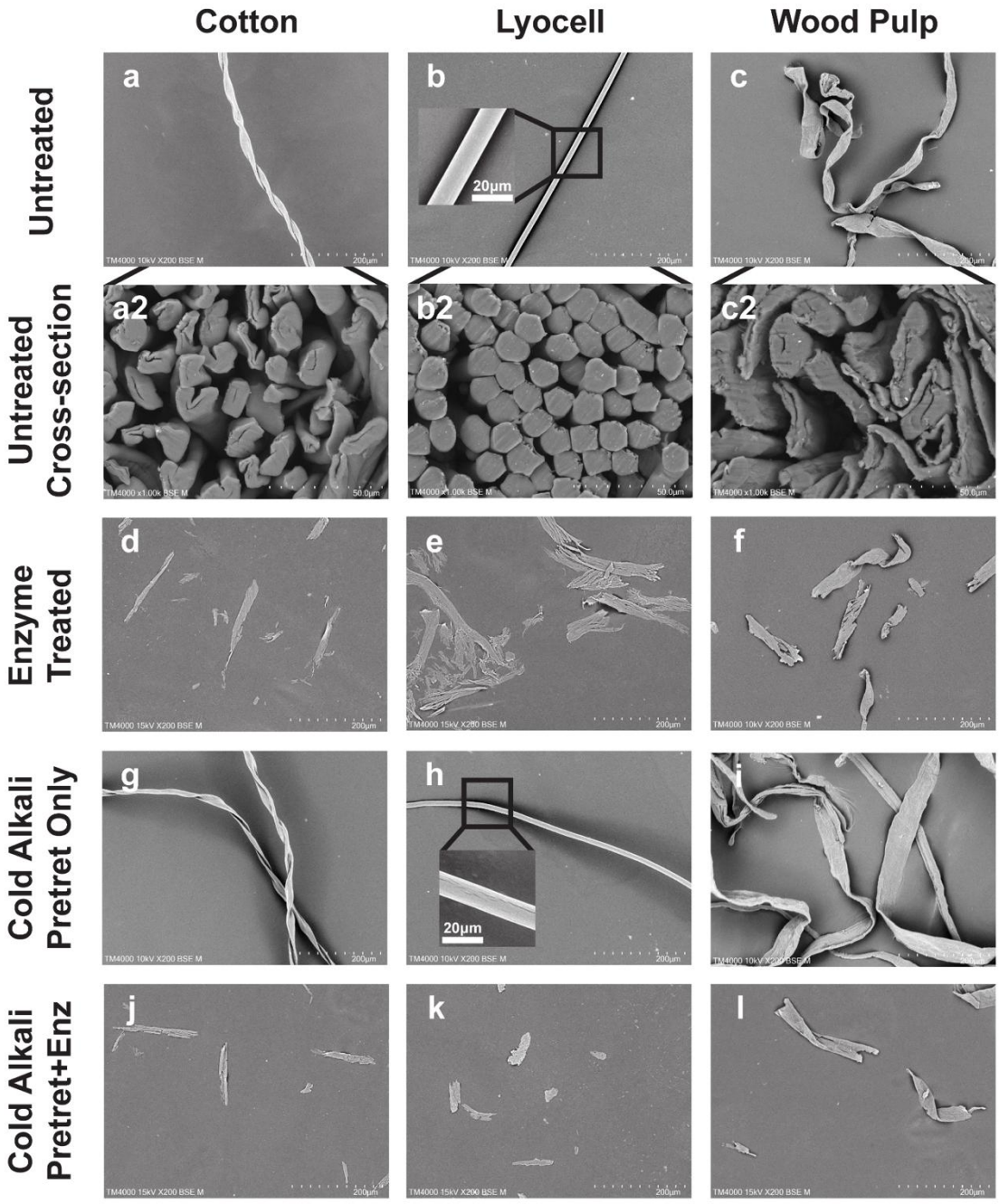

Fig. 3 SEM images of cellulose fibers (cotton, lyocell, and wood pulp) under different treatment conditions: (a-c) untreated fibers, (a2-c2) untreated fiber cross section, (d-f) residual small solids from enzyme-treated fibers (20 FPU/g, 20 h), (g-i) cold alkali pretreated fibers, and (j-l) residual small solids from fibers pretreated with cold alkali (g-i) followed by enzymatic hydrolysis (20 FPU/g, 20 h)

While cotton, lyocell, and wood pulp are all cellulose-based fibers, their morphologies and structural characteristics differ (**Fig. 3**). Untreated cotton fibers showed a characteristic twisted ribbon-like morphology formed from the collapsed

lumen when dried (**Fig. 3a**). This creates an uneven surface with an internal opening that may facilitate enzyme contact and promote fiber abrasion during mixing. Lyocell fibers exhibited a smoother and more uniform cylindrical morphology (**Fig. 3b**). In contrast, wood pulp fibers consisted of shorter, more collapsed (hornified, flat ribbon) and more entangled fibers (**Fig. 3c**). These morphological differences are expected to influence enzyme accessibility, fiber swelling, dispersion in aqueous media, and fragmentation behavior during enzymatic hydrolysis.

After enzymatic treatment, cotton and lyocell showed visible fibrillation and surface disintegration, including cracking and fragmentation into finer fiber residues (**Fig. 3d,e**). Wood pulp also showed fragmentation, but the remaining residues appeared larger and less fibrillated than cotton and lyocell (**Fig. 3f**), suggesting slower fiber disintegration. Cold alkali pretreatment alone did not change the bulk fiber appearances (**Fig. 3g,h,i** compared to **Fig. 3a,b,c**) though cracking along the surface of lyocell fiber occurred (Figure 3h). After alkali pretreatment followed by enzyme treatment, lyocell succumbed to such extensive breakdown that only a small amount of solid residues remained as small pieces rather than fibrous structure (**Fig. 3k**), indicating near complete degradation. Cotton also exhibited enhanced fragmentation after pretreatment, although some small resistant fragments remained (**Fig. 3j**). Wood pulp showed improved breakdown after pretreatment, with complete conversion of the residual large solids into small solid fragments and weight loss after 20 h. However, the remaining small solids still consisted of relatively larger fiber fragments (**Fig. 3l**) compared with cotton and lyocell, indicating that structural and morphological limitations continued to restrict complete hydrolysis.

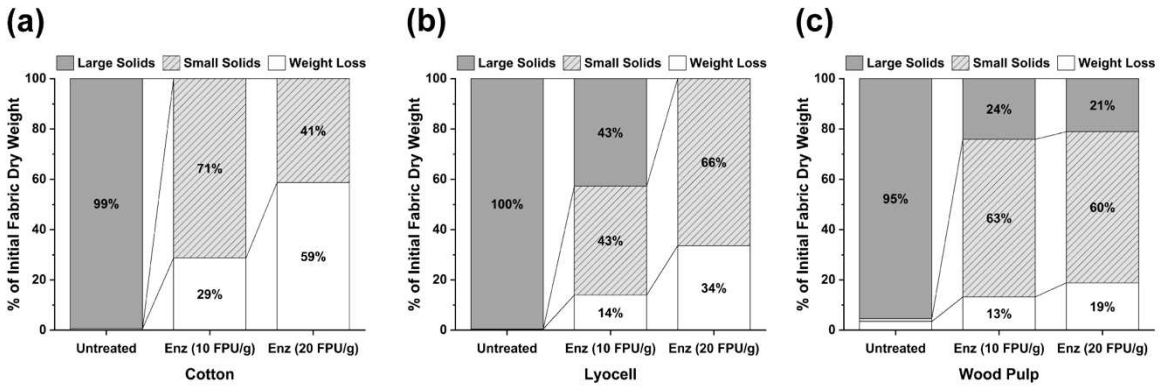

Fig. 4 Fiber type-dependent enzymatic degradation of cellulose fibers after 20 h at enzyme loadings of 10 and 20 FPU/g: (a) Cotton, (b) lyocell, and (c) wood pulp

Gravimetric analysis of the enzymatic degradation behavior also varied among cotton, lyocell, and wood pulp. As shown in **Fig. 4**, the distribution of large solids, small solid fragments, and weight loss differed across the three fiber types after 20 h of enzymatic treatment at enzyme loadings of 10 and 20 FPU/g. Since all three fibers are

primarily made up of cellulose polymer, these differences indicate that enzymatic degradation is governed not only by chemical composition but also by fiber morphology, enzyme accessibility, and crystalline structure.

For cotton fibers, no residual large solids remained after 20 h of enzymatic hydrolysis, even at the lower enzyme dosage of 10 FPU/g (**Fig. 4a**). Cotton showed the highest conversion to small solids at 10 FPU/g and the greatest overall weight loss among the three fibers. Weight loss increased from 29% to 59% with higher enzyme loading, indicating that higher enzyme dosage promoted further hydrolysis of cellulose into soluble sugars. The rapid disintegration of cotton fibers is attributed to their highly twisted ribbon-like morphology, uneven surface, and lumen structure, which likely enhances enzyme accessibility and mechanical mixing. These structural features allow enzymes to more effectively access easily soluble and less ordered regions compared to smoother, more compact fibers like lyocell. Notably, the presence of primary cell wall in this raw cotton sample did not prevent enzymatic degradation, though a prewetting step was required to fully saturate raw cotton with water before the degradation test.

Lyocell displayed a more gradual degradation behavior than cotton (**Fig. 4b**). At 10 FPU/g, 43% remained as large solids after 20 h, indicating limited initial enzyme accessibility. This behavior is attributed to the combination of smooth fiber surface and circular cross section that lead to low exposed surface area (Abu-Rous et al. 2006) and restrict enzyme penetration into the fiber interior. The limited permeability of the fiber surface may also be associated with anti-fibrillation treatments, such as crosslinking, which are used to reduce fibril separation in lyocell fibers (Ma et al. 2021). At the higher enzyme dosage of 20 FPU/g, degradation was accelerated, and no large solids remained after 20 h. Under this condition, lyocell reached 34% weight loss and 66% conversion to small solids. This strong enzyme dose dependence indicates that lyocell requires higher enzyme availability to overcome initial accessibility limitations.

Wood pulp exhibited the greatest resistance to enzymatic hydrolysis (**Fig. 4c**). Conversion to small solids and weight loss remained low under both enzyme dosages, and residual large solids remained after treatment. Under aqueous conditions, the fibers behaved similarly to their intended function in absorbent hygiene products by retaining water and forming swollen fiber aggregates (**Fig. S2**). This, combined with the short fiber length, likely reduced effective mechanical agitation and enzyme-fiber interactions. The role of short fiber length may seem counter-intuitive, but once fibers reach a certain short length, they can be small enough to evade physical impact from the mixing bars and no longer entangle each other leading to a slowing of degradation effects (Egan et al. 2023). Although wood pulp rapidly absorbs water, this does not necessarily indicate high enzyme accessibility within the fiber wall and pores. Water uptake can occur primarily through the capillary space between fibers, while the collapsed fiber wall may still limit internal swelling and restrict enzyme penetration into

cellulose microfibril regions. Consequently, enzyme accessibility rather than enzyme availability appears to be the primary limiting factor, which also explains the minimal improvement with increased enzyme dosage. In addition, the use of fluff pulp extracted from a commercial nonwoven product may further contribute to degradation resistance due to prior mechanical processing, drying history, or surface modifications.

Overall, the enzyme treatment results demonstrate a clear fiber-dependent degradation behavior. Cotton was the most readily fragmented and hydrolyzed, lyocell showed intermediate degradation with increased enzyme dosage, and wood pulp remained the most resistant. These results show that fiber morphology, crystalline structure, and dispersion behavior strongly influence cellulase accessibility and degradation efficiency.

Effect of Cold Alkali Pretreatment on Enzymatic Degradation Behavior

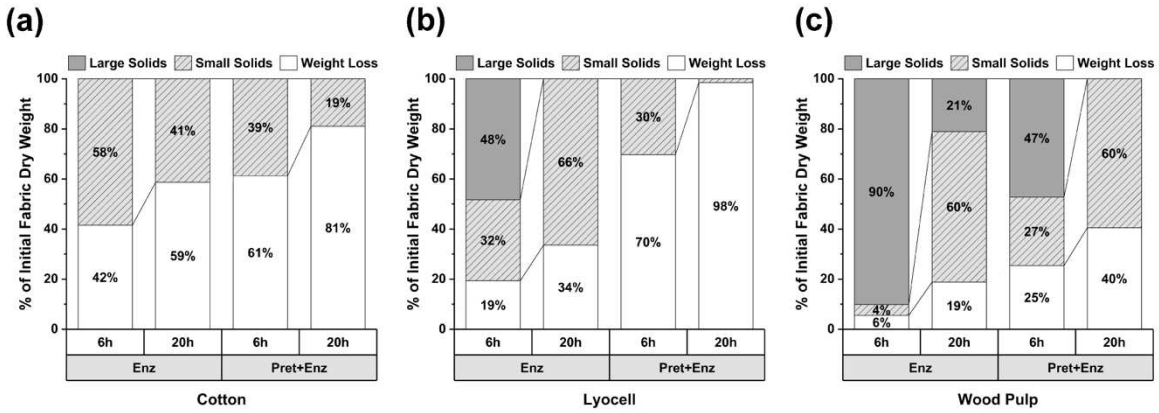

Fig. 5 Effect of cold alkali pretreatment on the enzymatic degradation behavior of cellulose fibers at 20 FPU/g. Comparison of hydrolysis at 6 h and 20 h for (a) cotton, (b) lyocell, and (c) wood pulp

Alkali pretreatment was applied to improve enzyme accessibility by swelling cellulose fibers, disrupting hydrogen bonding, and exposing less ordered regions. Three alkali pretreatment temperature conditions were initially investigated to compare fiber responses (**Fig. S3**). Cotton showed similar behavior across pretreatment conditions, lyocell showed greater degradation under cold alkali pretreatment, and wood pulp responded more strongly to hot conditions. Considering the overall response across the three fibers, cold alkali pretreatment was selected for further comparison at different reaction times (6 and 20 h).

As shown in **Fig. 5**, cold alkali pretreatment enhanced enzymatic degradation for all three fibers, but the effect depended strongly on fiber type. Pretreated fibers generally showed reduced residual large solids and increased small solids formation and weight loss compared with non-pretreated fibers. These results show that alkali pretreatment improved enzyme accessibility and enabled faster fiber breakdown.

For cotton fibers (**Fig. 5a**), no residual large solids remained even at the shorter treatment time of 6 h across all conditions, indicating rapid disintegration of the fiber structure. Cotton showed significant degradability even without pretreatment, while alkali pretreatment further increased weight loss. At 20 FPU/g after 20 h, non-pretreated cotton reached 59% weight loss, whereas alkali-pretreated cotton reached 81% weight loss under the same conditions. The weight loss of the pretreated sample at 6 h (61%) is higher than that of the non-pretreated sample at 20 h (59%). As cotton was already highly accessible, alkali pretreatment accelerated the early stages of hydrolysis and resulted in higher conversion of small solids fragments into soluble products.

Lyocell exhibited the most pronounced response to alkali pretreatment (**Fig. 5b**). Without pretreatment, lyocell was initially resistant to hydrolysis, with 92% (**Fig. S4b**) and 48% of large solids remaining after 6 h at 10 and 20 FPU/g, respectively. With an extended reaction time, lyocell gradually converted to smaller fragments. After alkali pretreatment, lyocell degraded rapidly even at early reaction times. The large solid fraction was eliminated after 6 h at 20 FPU/g and reached 98% weight loss after 20 h. This near-complete hydrolysis, combined with the evident cracking at the fiber surface (**Fig. 3h**), indicates that alkali pretreatment effectively disrupted the less permeable fiber skin and exposed the internal nanoporous structure (Abu-Rous et al. 2006) to cellulase, thereby increasing enzyme accessibility. The higher void volume associated with cellulose II morphology (Inglesby and Zeronian 2002) may further contribute to increased enzyme accessibility in the fiber core. (Ma et al. 2021). As a result, rapid and extensive hydrolysis occurred across reaction conditions.

Wood pulp remained the most resistant fiber, although pretreatment improved its degradability (**Fig. 5c**). Without pretreatment, almost no degradation occurred within 6h, with 90-92% remaining as large solids (**Fig. S4c**). Cold alkali pretreatment improved wood pulp breakdown, as pretreated fibers showed moderate breakdown even after 6 h, with 45-47% of the sample remaining as large solids and the rest converted to small solids or water-soluble sugars. After 20 h, no residual large solids remained, and the weight loss reached 30-40%. Although pretreatment accelerated hydrolysis compared with the non-pretreated condition, the overall weight loss remained lower than that of cotton and lyocell.

These results show that alkali pretreatment does not affect all cellulose fibers equally. Cotton showed enhanced solubilization despite already high enzyme accessibility, lyocell showed the greatest improvement due to disruption of its enzyme-resistant fiber “skin” structure, and wood pulp showed improved fragmentation but limited complete hydrolysis due to morphological restrictions.

Crystalline Structure Changes During Pretreatment and Enzymatic Hydrolysis

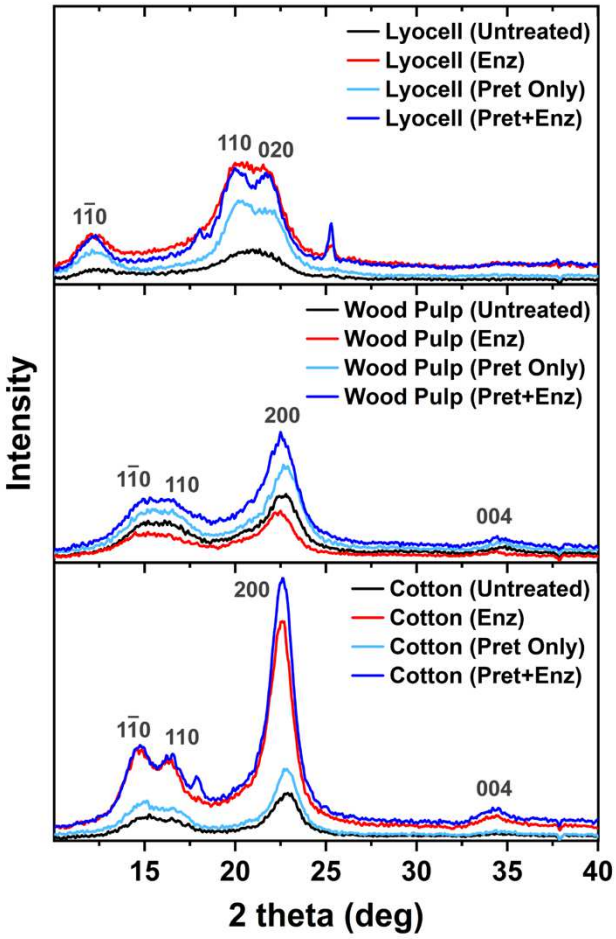

Fig. 6 X-ray diffraction (XRD) patterns of cellulose fibers (cotton, lyocell, and wood pulp) under different treatment conditions: untreated, enzyme-treated fibers (20 FPU/g, 20 h) (Enz), cold alkali pretreatment only (Pret Only), and cold alkali pretreatment followed by enzymatic hydrolysis (20 FPU/g, 20 h) (Pret+Enz)

Table 2 Crystallinity (X_c) of cellulose fibers under different treatment conditions

X_c (%)	Untreated	Pret Only	Enz	Pret+Enz
Cotton	73	73	79	76
Lyocell	63	51	72	74
Wood Pulp	64	65	67	67

X-ray diffraction (XRD) was used to characterize crystalline structure changes under different treatment conditions (**Fig. 6**). Cotton and wood pulp showed X-ray diffraction patterns characteristic of cellulose Iβ, with a major crystalline peak occurring at 2θ ≈ 22~23° corresponding to the plane (2 0 0). Additional peaks are the planes (1 -1 0) and (1 1 0) observed around 2θ ≈ 14~17°, with a minor peak for the (0 0 4) plane near 2θ ≈ 34.5°(French 2014). In contrast, lyocell showed diffraction patterns characteristic of cellulose II. The major crystalline peaks were observed at 2θ ≈ 22.1° corresponding to the plane (0 2 0), 2θ ≈ 20° for plane (1 1 0), and a minor peak for the (1 -1 0) plane near 2θ ≈ 12.2° (French 2014). The observed XRD pattern for lyocell aligns with reported values (Guo et al. 2021).

The crystallinity of the fibers under different treatment conditions was calculated using the integrated peak area method (**Table 2**). Enzymatic hydrolysis increased the crystallinity of the residual small solids for all three fibers, which is attributable to the removal of amorphous or less ordered cellulose regions. For cotton, X_c increased after enzymatic treatment, indicating that enzymes effectively removed accessible amorphous regions and what remained was harder to degrade crystalline regions. Cold alkali pretreatment alone resulted in no changes in crystallinity, as the NaOH concentration (1 M) was not high enough to significantly alter the crystalline structure. However, the combination of alkali pretreatment and enzymatic hydrolysis resulted in a slightly lower crystallinity (76%) compared to non-pretreated fragments. This suggests that pretreatment increased enzyme accessibility beyond the easily accessible amorphous regions, allowing partial disruption of more ordered domains. Also, as enzymatic hydrolysis proceeds, the removal of less ordered surface layers may expose more surface area of fragments with disrupted structural order and result in a slightly lower crystallinity in the residual solids.

Lyocell showed the most pronounced crystallinity changes among the three fibers. The crystallinity of lyocell decreased from 63% to 51% after cold alkali pretreatment. This reduction confirms the chain disordering from the swelling of the cellulose II structure. After enzymatic hydrolysis, crystallinity increased to 72% for the non-pretreated sample and further to 74% for the pretreated samples. The increase in crystallinity after enzymatic treatment reflects the removal of amorphous regions. The higher crystallinity of pretreated lyocell after hydrolysis aligns with its near-complete weight loss and suggests that most of the accessible cellulose has been removed, leaving only the most ordered residual fractions to be recovered as solids for analysis.

Wood pulp exhibited only slight variations in crystallinity across all treatment conditions. The minimal change in crystallinity indicates that the enzymatic hydrolysis of wood pulp mainly affects the accessible surface areas without significantly altering the overall crystalline structure. Cotton showed the fastest degradation, even though it has the highest crystallinity among the three fibers. In contrast, wood pulp displayed

the slowest degradation despite its lower crystallinity. This suggests that crystallinity is not the primary factor influencing enzymatic degradation behavior. Instead, morphological characteristics are more critical in determining enzyme accessibility. The lack of significant lignin peaks in the wood pulp from FTIR analysis (**Fig. S5**) confirms that chemical composition was not a restrictive factor for wood pulp. Thus, the lower degradability of wood pulp is primarily due to physical barriers, including fiber aggregation and restricted enzyme penetration.

The XRD results demonstrate that although the enzymatic hydrolysis trend aligns with the expected removal of the accessible amorphous regions, the overall degradation behavior of cellulose fibers is influenced by a combination of fiber morphology and crystalline structure. Specifically, alkali pretreatment significantly alters the fibrillar structure of lyocell, whereas the degradation behavior of wood pulp is primarily influenced by its morphological limitations.

Fragmentation Behavior of Residual Cellulose Particles

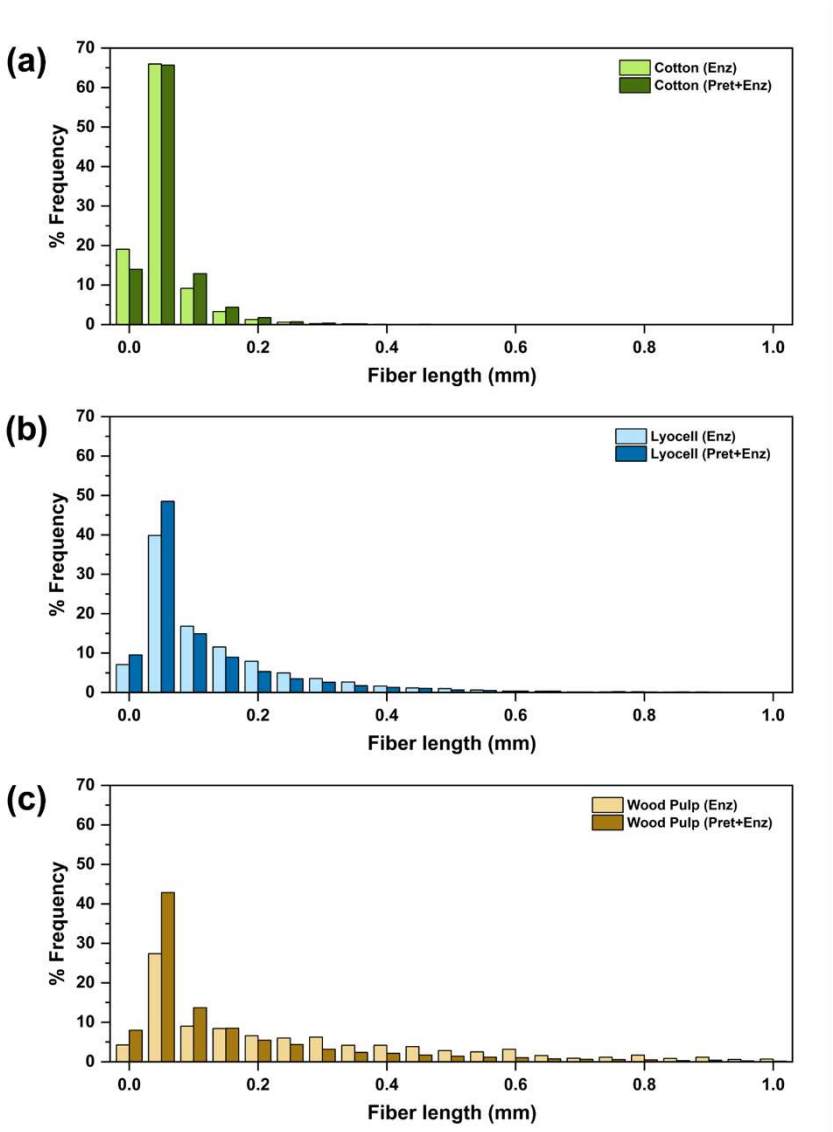

Fig. 7 FQA results (L_n) of cellulose fibers after enzyme treatment, enzyme-treated fibers (20 FPU/g, 20 h) (Enz) and cold alkali pretreatment followed by enzymatic hydrolysis (20 FPU/g, 20 h) (Pret+Enz): (a) cotton, (b) lyocell, and (c) wood pulp

Table 3 FQA results of the residual small solid fragments

	Arithmetic Length (L_n) (μm)	Length Weighted Length (L_w) (μm)	Width (μm)
Cotton (Enz)	77	181	22.8
Cotton (Pret+Enz)	80	111	21.5
Lyocell (Enz)	155	277	25.6
Lyocell (Pret+Enz)	135	264	23.1
Wood Pulp (Enz)	305	584	31.2
Wood Pulp (Pret+Enz)	180	397	31.7

Fiber quality analysis (FQA) was used to quantify the size distribution of residual small solids after enzymatic treatment, as the objective of hydrolysis is not necessarily complete saccharification, but fragmentation of cellulose into small dispersible particles that can be readily removed. Among the measured parameters, the length-weighted mean length (L_{lw}) is particularly important as it places greater emphasis on longer residual fragments while reducing the influence of fines (Li et al. 2011). Thus, L_{lw} provides insight into the effectiveness of fragmentation and the extent of residual fiber breakdown, with longer residual fragments indicating less complete fragmentation during hydrolysis.

The FQA results showed clear fiber-type-dependent differences in residual fragment size (**Table 3**). Cotton produced the smallest residual fragments after enzymatic treatment with L_n of 77-80 μm, and wood pulp produced the largest with L_n of 180-305 μm. These trends are consistent with the fiber length distribution in **Fig. 7**, where cotton exhibited the highest % frequency in the finer fragment sizes, while wood pulp showed a broader distribution extending toward larger fragment sizes.

The observed differences in fragmentation behavior can be attributed to the intrinsic morphology of each fiber. Cotton fiber, despite its relatively high crystallinity, has a long twisted ribbon morphology and structure that provides accessible regions for enzymes and mechanically enhanced degradation at multiple enzyme-weakened stress points. This allows rapid fiber breakdown and formation of finer fragments. Lyocell, with its smooth cylindrical morphology and dense "skin" structure, has a smaller accessible surface area, leading to more gradual fragmentation and larger residual fragments compared with cotton. Wood pulp retained larger fragments after enzymatic hydrolysis, likely due to fiber aggregation and entanglement, which restricts enzyme access within swollen fiber clusters and minimized benefits of mechanical agitation.

Furthermore, alkali pretreatment also influenced fragmentation behavior differently across the fibers. For lyocell and wood pulp, pretreatment reduced both L_n and L_{lw}. This confirms that pretreatment enhanced fragmentation and production of finer residues. Cotton showed a slightly higher L_n after pretreatment, increasing from 77 to 80 μm. This slight increase does not indicate reduced degradation, as the arithmetic mean is dominated by the most frequent small particle size ranges, and fragments below the FQA detection range (<40 μm) may not be fully represented. More importantly, the L_{lw} decreased substantially from 181 to 111 μm after pretreatment, which shows a strong reduction in longer residual fragments. Thus, pretreatment reduced the fraction of larger residual fragments and resulted in more uniform fragmentation of cotton fibers.

Overall, FQA results confirm that residual fragment size distribution is also an important evaluation factor for enzymatic degradation. Especially for cellulose/PET separation, reducing longer residual cellulose fragments is important, as smaller and more dispersible cellulose particles are more easily removed from the blended textile.

Fiber structure-dependent degradation mechanism

The combined experimental results provide mechanistic insight into the fiber-dependent degradation behavior illustrated in **Fig. 2** and summarized in **Table 4**. The degradation behavior of cellulose fibers is governed by the combined effects of fiber morphology, fibrillar structure, dispersion behavior in aqueous media, crystalline structure and susceptibility to mechanical stress during agitation.

Cotton showed fastest degradation because its twisted ribbon-like morphology from the collapsed lumen structure and uneven surface provided high enzyme accessibility and mechanical agitation during mixing. Despite its relatively high crystallinity, these structural characteristics enabled rapid conversion into small solids fragments and soluble sugars. Alkali pretreatment further enhanced hydrolysis by improving access to less accessible regions and producing shorter small solids fragments.

Lyocell initially exhibited slower degradation because its smooth skin surface limited enzyme accessibility. However, alkali pretreatment disrupted the outer skin and promoted access to the more readily degradable core. The highly oriented fibrillar structure and relatively low lateral cohesion of lyocell facilitate fibril separation during swelling (Jiang et al. 2020), exposing additional cellulose fiber surfaces to enzymes. This increased enzyme accessibility is consistent with the fibrillation observed by SEM (**Figure 3e**) and the near-complete hydrolysis achieved after enzymatic treatment.

Wood pulp showed the greatest resistance to enzymatic degradation due to its short, collapsed, hornified, and highly entangled morphology. Rapid water absorption promoted the formation of swollen fiber aggregates that reduced mixing efficiency and limited enzyme contact throughout the fiber. Although alkali pretreatment improved fragmentation, overall hydrolysis remained lower than that of cotton and lyocell. This indicates that enzymatic hydrolysis of wood pulp is governed primarily by physical accessibility and fiber dispersion.

Table 4 Summary of fiber structure-dependent enzymatic degradation behavior.

Cellulose fiber	Water Absorption	Mixing Behavior	Enzyme accessibility	Enzymatic Hydrolysis	Degradation Mechanism	Residual Fragments
Cotton	Slow initial wetting (surface waxes)	Good	High	Rapid	Unwrapping and fibrillation	Minimal
Lyocell	Rapid wetting	Good	Low	Limited initially, rapid after alkali pretreatment	Fibrillation	Small fiber fragments
Wood Pulp	Rapid swelling	Aggregate (poor dispersion)	Low	Slow	Transverse cracking and fragmentation	Large fiber fragments

Conclusions

The enzymatic degradation behavior of three cellulose fibers, cotton, lyocell, and wood pulp, was investigated under enzymatic and alkaline pretreatment conditions. Distinct degradation behaviors were observed among the fibers, including differences in hydrolysis rate, fiber fragmentation, residual fiber fragment morphology, and crystallinity change. Alkali pretreatment significantly enhanced degradation,

particularly for lyocell, while cotton exhibited high inherent degradability even without pretreatment. In contrast, wood pulp showed the greatest resistance to hydrolysis and retained larger residual fiber fragments despite pretreatment.

Enzymatic degradation behavior is strongly dependent on intrinsic fiber morphology and structural accessibility rather than crystallinity alone. Although cotton has the highest crystallinity, its accessible fibrillar structure enabled rapid fragmentation and hydrolysis. Lyocell initially showed limited enzyme accessibility due to its smooth impermeable “skin” surface, but alkaline pretreatment effectively disrupted the fibrillar arrangement and enabled near complete degradation. Wood pulp degradation remained limited due to collapsed fiber morphology and fiber aggregation, which restricted enzyme penetration and reduced effective fragmentation.

Direct comparison of structurally distinct cellulose fibers under identical hydrolysis conditions highlights the importance of fiber-dependent fragmentation behavior during enzymatic treatment. Unlike conventional approaches focused on complete saccharification, this work emphasizes controlled fiber fragmentation as a practical pathway for cellulose removal in textile recycling and nonwoven waste management. These findings provide a structural foundation for understanding and optimizing enzymatic degradation behavior in a more complex cellulose/PET blended textile system. Ongoing work will extend this approach to cellulose/PET nonwovens to investigate the influence of cellulose fiber type and nonwoven structure on cellulose removal and material separation.

Statements & Declarations

Funding

This research was supported by a grant from the Korea Institute for Advancement of Technology (KIAT), funded by the Ministry of Trade, Industry and Energy (MOTIE, Korea) (No. P0028353).

Competing Interests

The authors have no relevant financial or non-financial interests to disclose.

Author contributions

All authors contributed to the study conception and design. Material preparation, data collection and analysis were performed by Jeongmin Oh. The first draft of the manuscript was written by Jeongmin Oh and all authors commented on previous versions of the manuscript. All authors read and approved the final manuscript.

References

Abu-Rous M, Ingolic E, Schuster KC (2006) Visualisation of the fibrillar and pore morphology of cellulosic fibres applying transmission electron microscopy. Cellulose 13(4):411–419. https://doi.org/10.1007/s10570-006-9052-5

ASTM (2018) ASTM D5103-07 Standard Test Method for Length and Length Distribution of Manufactured Staple Fibers (Single-Fiber Test)

Bajpai P (2018) Biermann's Handbook of Pulp and Paper: Volume 1: Raw Material and Pulp Making. Elsevier

Barnett JR, Bonham VA (2004) Cellulose microfibril angle in the cell wall of wood fibres. Biol. Rev. Camb. Philos. Soc. 79:461–472

Boondaeng A, Keabpimai J, Srichola P, Vaithanomsat P, Trakunjae C, Niyomvong N (2023) Optimization of Textile Waste Blends of Cotton and PET by Enzymatic Hydrolysis with Reusable Chemical Pretreatment. Polymers (Basel) 15(8). https://doi.org/10.3390/polym15081964

Cho EJ, Lee YG, Song Y, Kim HY, Nguyen DT, Bae HJ (2023) Converting textile waste into value-added chemicals: An integrated bio-refinery process. Environmental Science and Ecotechnology 15. https://doi.org/10.1016/j.ese.2023.100238

Costa C, Viana A, Silva C, Marques EF, Azoia NG (2022) Recycling of textile wastes, by acid hydrolysis, into new cellulosic raw materials. Waste Management 153:99–109. https://doi.org/10.1016/j.wasman.2022.08.019

De Silva R, Wang X, Byrne N (2014) Recycling textiles: The use of ionic liquids in the separation of cotton polyester blends. RSC Adv 4(55):29094–29098. https://doi.org/10.1039/c4ra04306e

EDANA (2019) EDANA Sustainability report 2019

Egan J, Wang S, Shen J, Baars O, Moxley G, Salmon S (2023) Enzymatic textile fiber separation for sustainable waste processing. Resources, Environment and Sustainability 13. https://doi.org/10.1016/j.resenv.2023.100118

Enking J, Becker A, Schu G, Gausmann M, Cucurachi S, Tukker A, Gries T (2025) Recycling processes of polyester-containing textile waste–A review. Resour. Conserv. Recycl. 219

French AD (2014) Idealized powder diffraction patterns for cellulose polymorphs. Cellulose 21(2):885–896. https://doi.org/10.1007/s10570-013-0030-4

Gritsch SM, Mihalyi S, Bartl A, Ipsmiller W, Jenull-Halver U, Putz RF, Quartinello F, Guebitz GM (2023) Closing the cycle: Enzymatic recovery of high purity glucose and

712 polyester from textile blends. Resour Conserv Recycl 188.
713 https://doi.org/10.1016/j.resconrec.2022.106701

714 Guo Y, Xiao M, Ren Y, Liu Y, Wang Y, Guo X, Liu X (2021) Synthesis of an effective
715 halogen-free flame retardant rich in phosphorus and nitrogen for lyocell fabric.
716 Cellulose 28(11):7355–7372. https://doi.org/10.1007/s10570-021-03975-8

717 Haigler CH, Betancur L, Stiff MR, Tuttle JR (2012) Cotton fiber: A powerful single-cell
718 model for cell wall and cellulose research. Front. Plant Sci. 3

719 Hinchliffe DJ, Thyssen GN, Condon BD, Zeng L, Hron RJ, Madison CA, Jenkins JN,
720 McCarty JC, Delhom CD, Sui R (2023) Interrelationships between cotton fiber
721 quality traits and tensile properties of hydroentangled nonwoven fabrics. Journal of
722 Industrial Textiles 53. https://doi.org/10.1177/15280837231171312

723 Huang X, Tan Y, Huang J, Zhu G, Yin R, Tao X, Tian X (2024) Industrialization of open- and
724 closed-loop waste textile recycling towards sustainability: A review. J. Clean. Prod.
725 436

726 Hubbe MA, Venditti RA, Rojas OJ (2007) How fibers change in use, recycling

727 Inglesby MK, Zeronian SH (2002) Direct dyes as molecular sensors to characterize
728 cellulose substrates. Cellulose 9(1):19–29.
729 https://doi.org/https://doi.org/10.1023/A:1015840111614

730 Isogai A, Atalla RH (1998) Dissolution of cellulose in aqueous NaOH solutions.
731 Cellulose 5(4):309–319

732 Jeihanipour A, Karimi K, Niklasson C, Taherzadeh MJ (2010) A novel process for ethanol
733 or biogas production from cellulose in blended-fibers waste textiles. Waste
734 Management 30(12):2504–2509. https://doi.org/10.1016/j.wasman.2010.06.026

735 Jiang X, Bai Y, Chen X, Liu W (2020) A review on raw materials, commercial production
736 and properties of lyocell fiber. Journal of Bioresources and Bioproducts 5:16–25

737 Joseph ML (1986) Introductory textile science. Holt, Rinehart and Winston

738 Kaabel S, Arciszewski J, Borchers TH, Therien JPD, Friščić T, Auclair K (2023) Solid-State
739 Enzymatic Hydrolysis of Mixed PET/Cotton Textiles**. ChemSusChem 16(1).
740 https://doi.org/10.1002/cssc.202201613

741 Kakonke G, Tesfaye T, Sithole B, Ntunka M (2019) Iss 1 Review on the Manufacturing and
742 Properties of Nonwoven Superabsorbent Core Fabrics used in Disposable Diapers.
743 International Journal of Chemical Sciences Review | 17(1):302.
744 https://doi.org/10.21767/0972-768X.1000300

745 Leenders N, van Klink GPM, Gruter GJM (2025) Towards polycotton waste valorisation:
746 depolymerisation of cotton to glucose with polyester preservation. RSC
747 Sustainability 3:3863–3882

748 Lenzing AG (2026) LenzingPro Product Catalog: Lyocell Fibers. https://lenzingpro.com.
749 Accessed 5 Aug 2026

750 Li B, Bandekar R, Zha Q, Alsaggaf A, Ni Y (2011) Fiber quality analysis: OpTest fiber
751 quality analyzer versus L&W fiber tester. Ind Eng Chem Res 50(22):12572–12578.
752 https://doi.org/10.1021/ie201631q

753 Li X, Hu Y, Du C, Lin CSK (2019) Recovery of Glucose and Polyester from Textile Waste by
754 Enzymatic Hydrolysis. Waste Biomass Valorization 10(12):3763–3772.
755 https://doi.org/10.1007/s12649-018-0483-7

756 Liu W, Liu S, Liu T, Liu T, Zhang J, Liu H (2019) Eco-friendly post-consumer cotton waste
757 recycling for regenerated cellulose fibers. Carbohydr Polym 206:141–148.
758 https://doi.org/10.1016/j.carbpol.2018.10.046

759 Ma J, Yang K, Wang M, Shan J, Yang D, Tian G (2024) Advancements in component
760 separation through chemical methods for recycled polyester/cotton blended
761 textiles. Cellulose 31:9543–9563

762 Ma Y, Rissanen M, You X, Moriam K, Hummel M, Sixta H (2021) New method for
763 determining the degree of fibrillation of regenerated cellulose fibres. Cellulose
764 28(1):31–44. https://doi.org/https://doi.org/10.1007/s10570-020-03513-y

765 Moon RJ, Martini A, Nairn J, Simonsen J, Youngblood J (2011) Cellulose nanomaterials
766 review: Structure, properties and nanocomposites. Chem Soc Rev 40(7):3941–
767 3994. https://doi.org/10.1039/c0cs00108b

768 Nam S, Slopek R, Wolf D, Warnock M, Condon BD, Sawhney P, Gbur E, Reynolds M,
769 Allen C (2016) Comparison of biodegradation of low-weight hydroentangled raw
770 cotton nonwoven fabric and that of commonly used disposable nonwoven fabrics
771 in aerobic Captina silt loam soil. Textile Research Journal 86(2):155–166.
772 https://doi.org/10.1177/0040517514551468

773 Ruiz-Caldas MX, Carlsson J, Sadiktsis I, Jaworski A, Nilsson U, Mathew AP (2022)
774 Cellulose Nanocrystals from Postconsumer Cotton and Blended Fabrics: A Study
775 on Their Properties, Chemical Composition, and Process Efficiency. ACS Sustain
776 Chem Eng 10(11):3787–3798. https://doi.org/10.1021/acssuschemeng.2c00797

777 Santos AS, Ferreira PJT, Maloney T (2021) Bio-based materials for nonwovens. Cellulose
778 28(14):8939–8969

779 Sasaki C, Nakagawa T, Asada C, Nakamura Y (2020) Microwave-Assisted Hydrolysis of
780 Cotton Waste to Glucose in Combination with the Concentrated Sulfuric Acid

781 Impregnation Method. Waste Biomass Valorization 11(8):4279–4287.
782 https://doi.org/10.1007/s12649-019-00768-w

783 Sawhney APS, Condon B, Reynolds M, Slopek R, Hui D (2010) Advent of Greige Cotton
784 Non-Wovens Made using a Hydro-Entanglement Process. Textile Research Journal
785 80(15):1540–1549. https://doi.org/10.1177/0040517510363194

786 Schindler WD, Hauser PJ (2004) Chemical finishing of textiles. Elsevier

787 Shen F, Xiao W, Lin L, Yang G, Zhang Y, Deng S (2013) Enzymatic saccharification
788 coupling with polyester recovery from cotton-based waste textiles by phosphoric
789 acid pretreatment. Bioresour Technol 130:248–255.
790 https://doi.org/10.1016/j.biortech.2012.12.025

791 Simonetti M, Butti P, Di Lorenzo RD, Mapelli V, Branduardi P (2024) Valorisation of cotton
792 post-industrial textile waste into lactic acid: chemo-mechanical pretreatment,
793 separate hydrolysis and fermentation using engineered yeast. Microb Cell Fact
794 23(1). https://doi.org/10.1186/s12934-024-02384-3

795 Smithers (2025) The Future Of Global Nonwovens To 2030.
796 https://www.smithers.com/services/market-reports/nonwovens/the-future-of-
797 global-nonwovens-to-2030. Accessed 20 Aug 2026

798 Smook GA (2016) Handbook for Pulp & Paper Technologists, 4th, illustrated edn. Tappi
799 Press

800 Textile Exchange (2025) Textile Exchange Materials Materials Market Report 2025

801 Vera RE, Suarez A, Zambrano F, Marquez R, Bedard J, Vivas KA, Pifano A, Farrell M,
802 Ankeny M, Jameel H, Gonzalez R (2023) Upcycling cotton textile waste into bio-
803 based building blocks through an environmentally friendly and high-yield
804 conversion process. Resour Conserv Recycl 189.
805 https://doi.org/10.1016/j.resconrec.2022.106715

806 Wakelyn PJ, Bertoniere NR, French AD, Thibodeaux DP, Triplett BA, Rousselle M-A,
807 Goynes JR, Edwards JV, Hunter L, McAlister DD (2006) Cotton fiber chemistry and
808 technology. CRC Press

809 Yang K, Wang M, Wang X, Shan J, Zhang J, Tian G, Yang D, Ma J (2024) Polyester/Cotton-
810 Blended Textile Waste Fiber Separation and Regeneration via a Green Chemistry
811 Approach. ACS Sustain Chem Eng 12(11):4530–4538.
812 https://doi.org/10.1021/acssuschemeng.3c07707

813 Zhang J, Wu J, Yu J, Zhang X, He J, Zhang J (2017) Application of ionic liquids for
814 dissolving cellulose and fabricating cellulose-based materials: State of the art and
815 future trends. Mater. Chem. Front. 1:1273–1290

816 Zhang S, Chen C, Duan C, Hu H, Li H, Li J, Liu Y, Ma X, Stavik J, Ni Y (2018) Regenerated
817 cellulose by the lyocell process, a brief review of the process and properties.
818 Bioresources 13(2):4577–4592

819 Zhang YHP, Lynd LR (2004) Toward an aggregated understanding of enzymatic hydrolysis
820 of cellulose: Noncomplexed cellulase systems. Biotechnol. Bioeng. 88:797–824

821

822

Supplementary Files

This is a list of supplementary files associated with this preprint. Click to download.

- SIEnzymaticDegradationBehaviorofCottonLyocellandWoodPulp20260923.pdf